

## A 43-Nucleotide RNA *Cis*-Acting Element Governs the Site-Specific Formation of the 3' End of a Poxvirus Late mRNA

Susan T. Howard,<sup>1</sup> Caroline A. Ray, Dhavalkumar D. Patel, James B. Antczak,<sup>2</sup> and David J. Pickup<sup>3</sup>

Department of Microbiology, Duke University Medical Center, Durham, North Carolina 27710

Received November 2, 1998; returned to author for revision November 17, 1998; accepted November 30, 1998

The 3' ends of late mRNAs of the *ati* gene, encoding the major component of the A-type inclusions, are generated by endoribonucleolytic cleavage at a specific site in the primary transcript [Antczak *et al.*, (1992), *Proc. Natl. Acad. Sci. USA* 89, 12033–12037]. In this study, sequence analysis of cDNAs of the 3' ends of *ati* mRNAs showed these mRNAs are 3' polyadenylated at the RNA cleavage site. This suggests that *ati* mRNA 3' end formation involves cleavage of a late transcript, with subsequent 3' polyadenylation of the 5' cleavage product. The RNA *cis*-acting element, the AX element, directing orientation-dependent formation of these mRNA 3' ends, was mapped to a 345-bp *AluI*-*XbaI* fragment. Deletion analyses of this fragment showed that the boundaries of the AX element are within –5 and +38 of the RNA cleavage site. Scanning mutagenesis showed that the AX element contains at least two subelements: subelement I, 5'-UUUUAU ↓ CCGAUAAUUC-3', containing the cleavage site (↓), separated from the downstream subelement II, 5'-AAUUUCGGAUUUGAAUGC-3', by a 10-nucleotide region, whose composition may be altered without effect on RNA 3' end formation. These features, which differ from those of other elements controlling RNA processing, suggest that the AX element is a component of a novel mechanism of RNA 3' end formation. © 1999 Academic Press

### INTRODUCTION

The mechanisms by which the 3' ends of mature poxviral late RNAs are generated are not fully understood. The poxviruses primarily use viral enzymes, including a multisubunit RNA polymerase resembling RNA polymerase II, to transcribe their DNA genomes in the cytoplasm of infected cells (reviewed by Moss, 1996). Consequently, the mechanisms of 3' end formation of viral RNAs may be independent of those generating the 3' ends of host cell RNAs.

During the early phase of viral replication, the 3' ends of mRNAs are generated by the termination of transcription (Rohrmann *et al.*, 1986). This event is governed by the *cis*-acting element UUUUUNU in the RNA and by termination factors, including the capping enzyme and the virus-encoded nucleoside triphosphate phosphohydrolase I (Deng *et al.*, 1996; Deng and Shuman, 1996, 1998; Shuman *et al.*, 1987; Shuman and Moss, 1988; Yuen and Moss, 1987). However, this transcriptional termination mechanism does not appear to be operational during late transcription (Weinrich and Hruby, 1987; Weir and Moss, 1984).

The viral late mRNAs present in virus-infected cells are often heterogeneous in length, with mRNAs of certain genes frequently exhibiting lengths ranging from just longer than the open reading frame to several kilobases longer than this (Mahr and Roberts, 1984; Weinrich *et al.*, 1985; Weir and Moss, 1984). It is unclear whether these heterogeneous length RNAs are primary transcription products, post-transcriptionally processed RNAs, or both, together with partially degraded RNAs. Other characterized viral late RNAs, such as those encoding the major protein component of the A-type inclusions (Amegadzie *et al.*, 1992; Patel and Pickup, 1987), those encoding the second-largest subunit of the RNA polymerase (Patel and Pickup, 1989), and the late telomeric transcripts (Parsons and Pickup, 1990), are homogeneous in length, with each having defined 3' ends. This homogeneity suggested that the 3' ends of each of these late RNAs are generated by the termination of transcription, by site-specific RNA processing, or by a combination of the two mechanisms.

Analyses of the mechanism of 3' end formation of the late mRNAs encoding the major protein component of the A-type inclusions (in cowpox virus, the 160-kDa protein encoded by the *ati* gene) showed that these 3' ends are generated by site-specific RNA cleavage (Antczak *et al.*, 1992). This result suggested that these and other viral late RNAs may form their 3' ends by a process similar to that generating the 3' ends of mRNAs generated by host cell transcription, namely, by a process involving site-specific RNA cleavage followed by 3' polyadenylation. In

<sup>1</sup> Current address: Department of Hematology and Oncology, School of Medicine, University of New Mexico, Albuquerque, NM 87131.

<sup>2</sup> Current address: Trimeris, 4727 University Drive, Durham, NC 27707.

<sup>3</sup> To whom reprint requests should be addressed at Box 3020. Fax: 919-684-8735. E-mail: pickup@abacus.mc.duke.edu.

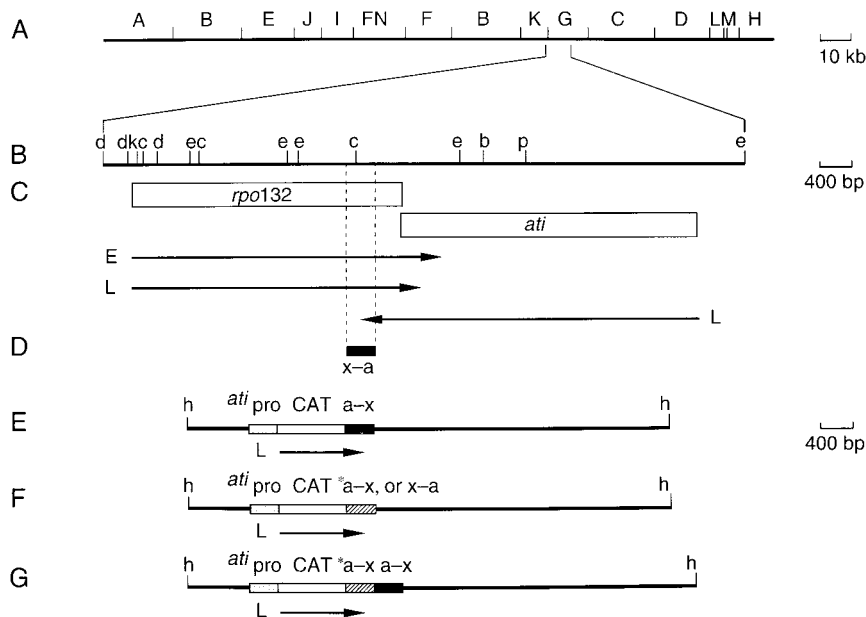


**FIG. 1.** Position of the *ati* gene and the AX element in the cowpox virus genome. (A) *KpnI* restriction map of the genome of the Brighton Red strain of cowpox virus (Archard *et al.*, 1984; Pickup *et al.*, 1984). (B) Restriction map of a 7.8-kb fragment of CPV-BR, which overlaps the *KpnI* K-G junction. Restriction sites are abbreviated as follows: b, *Bam*HI; c, *Cla*I; d, *Dra*I; e, *Eco*RI; k, *Kpn*I; and p, *Pst*I. (C) Transcriptional map of the *rpo132* and *ati* genes. The *rpo132* gene encodes the second largest subunit of the viral DNA-dependent RNA polymerase. This gene is located immediately downstream of the *ati* gene (Amegadzie *et al.*, 1991; Patel and Pickup; 1987, 1989). The positions of the coding regions of the two genes are indicated by rectangles. The arrows represent the transcribed regions: E, at early times after infection; and L, at late times after infection. The tail of each arrow corresponds to the beginning of a transcribed region. The arrowhead of the late *ati* gene transcription unit corresponds to the extent of complementarity between the defined 3' ends of the transcript (when detectable) and the viral DNA. The arrowhead of the late *rpo132* transcripts corresponds to the position of one of the major 3' ends of these transcripts (Patel and Pickup, 1989). (D) A 345-bp *AluI-XbaI* fragment (a-x) contains the element designated AX that directs 3' end formation in RNAs of the *ati* gene. (E and F) Maps of the *HindIII J* fragments of the genomes of the WR strain of vaccinia virus after these fragments have been modified to contain a copy of CAT gene (under the transcriptional control of the late promoter of the *ati* gene) inserted in the TK gene. In these constructs, (E) the 345-bp *AluI-XbaI* fragment (a-x) containing the AX element is downstream of the CAT gene. (F) The 345-bp *AluI-XbaI* fragment containing 5' deletions, 3' deletions, or scanning mutations of the AX element (\*a-x) is downstream of the CAT gene, or the 345-bp *AluI-XbaI* fragment was placed in an orientation opposite to that in which it is found downstream of the *ati* gene (x-a). (G) In one recombinant, there was a partial duplication of the 345-bp *AluI-XbaI* fragment such that the construct contained one complete copy of the fragment inserted in tandem downstream of an *AluI-NsiI* subfragment (-50 to +196; see Fig. 2).

this process, the formation of the 3' ends of host RNA polymerase II transcripts is directed by *cis*-acting elements typically composed of a consensus polyadenylation signal, AAUAAA, 10–30 nucleotides upstream of the cleavage site, and a U- or GU-rich sequence, 20–40 nucleotides downstream of the cleavage site (reviewed by Colgan and Manley, 1997; Wahle and Keller, 1996).

In this study, we characterized the *cis*-acting element directing formation of the 3' ends of the *ati* mRNAs. We show that the *cis*-acting element of the viral RNA required for 3' end formation is composed of at least two noncontiguous subelements, most of which are downstream of the cleavage site. In these properties, the viral sequences are similar to the *cis*-acting elements directing 3' end formation of RNA polymerase II transcripts. However, the sequence composition of the viral *cis*-acting element is unlike those of any other elements known to direct either RNA 3' end formation, or RNA processing, suggesting this viral RNA element is a component of a novel mechanism of RNA 3' formation.

## RESULTS

### Characterization of the sequences at the 3' ends of the *ati* mRNAs

The 3' ends of the *ati* mRNAs map to a site within a 345-bp *AluI-XbaI* fragment contained within the coding region of the convergently transcribed *rpo132* gene, as shown in Fig. 1 (Patel and Pickup, 1987). Subsequent studies using primer extension and S1 nuclease protection analyses had indicated that *in vitro* cleavage of precursor *ati* RNAs occurred after the sequence 5'-UUUUAU-3', between the nucleotides designated -1 and +1 in Fig. 2 (Antczak *et al.*, 1992). These results were consistent with the homogeneous nature of the 3' ends that had been suggested by the earlier RNA hybridization analyses of RNAs from virus-infected cells. There was no indication from either analysis that any significant proportion of the RNAs had 3' ends corresponding to alternative positions within ~200 nucleotides of the identified end point.

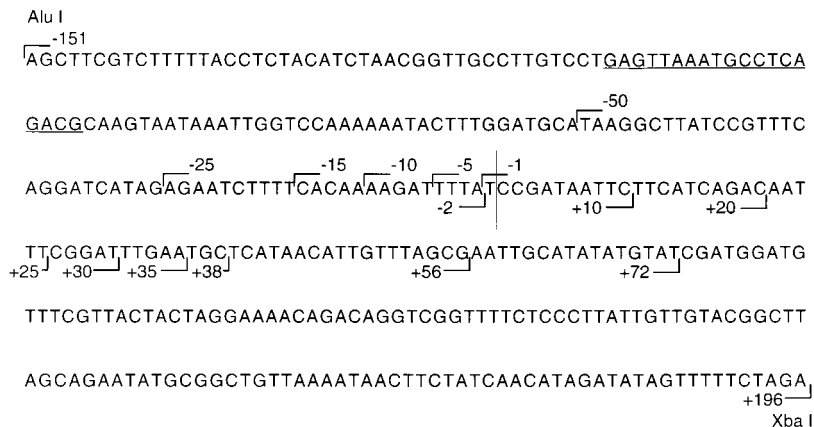


**FIG. 2.** Nucleotide sequence of the *AluI*-*XbaI* fragment containing the AX element. The sequence of the noncoding strand of the *rpo132* gene is shown (Patel and Pickup, 1989). The underlined sequence corresponds to part of the sequence of the primer 160KPS used to obtain cDNA copies of the 3' end of mRNAs of the *ati* gene. The vertical bar corresponds to the position of the cleavage in the RNA version of this fragment (Antczak *et al.*, 1992). Nucleotides are numbered with respect to the position of the cleavage site (i.e., nucleotides upstream of the cleavage site are numbered -1 to -151 and those downstream are numbered +1 to +196). With respect to the mutational analyses of this sequence, the end points of the 5' deletions are shown above the sequence, and the end points of 3' deletions of this fragment are shown below the sequence (inclusive numbering as indicated by each bracket).

Although these analyses provided a good indication of the end points of complementarity between the majority of the *ati* RNAs and the DNA, and the position of the cleavage site, they had two limitations. First, the S1 nuclease protection assay had identified the 3' ends to a region of four nucleotides. However, it was unclear whether this result reflected actual heterogeneity in 3' ends or the partial nuclease sensitivity of the four nucleotides next to the junction of complementarity between the 3' polyadenylated RNAs and the DNA probe. Second, these analyses could not provide any information on the presence or nature of any sequences in the cleaved RNA downstream of the cleavage site. The lengths of the *ati* RNAs suggested the presence of 3' poly(A) tails, but the ability of these RNAs to hybridize with oligo(dT) cellulose could not demonstrate this definitively because of the presence of 5' poly(A) sequences in these RNAs (Patel and Pickup, 1987). Therefore, to gain more precise information on the nature of the 3' ends of these late RNAs, the nucleotide sequences of cDNAs derived from the 3' ends of *ati* RNAs of both cowpox virus and vaccinia virus were determined.

The cDNAs were generated according to the rapid amplification of cDNA ends (RACE) procedure (Frohman, 1990; Frohman *et al.*, 1988) in which the synthesis of the first strand of the cDNA was initiated from an oligo(dT)-containing primer designed to anneal with the 3' poly(A) tail. The success of this procedure demonstrated that *ati* RNAs possessed 3' poly(A) tails. The cDNAs derived from the 3' ends of *ati* mRNAs were amplified by PCR. The majority of the PCR products were ~130–250 bp long, consistent with the length between the position of the sequence complementary to the 160KPS primer and the end point of complementarity between the RNA and the DNA (Fig. 2), plus some base pairs from the 3' poly(A)

tail. The amplified cDNAs were fractionated by gel electrophoresis (eight fractions containing DNAs 125–600 bp long). The DNAs in each fraction were separately ligated into the plasmid vector pGEM3Z, and the products of the ligations were used to transform *Escherichia coli* JM109 cells. Plasmid DNAs from 36 transformants selected at random from each of the eight groups of transformants were analyzed by restriction enzyme cleavage with *PstI* and *XbaI*. Inserts were detected that ranged in size from ~145 to 210 bp, consistent with the lengths of the major products of the PCR amplification. However, plasmids with inserts similar in length to some of the longer (210–600 bp), but less abundant, products of the PCR amplification were not recovered.

The nucleotide sequences of 20 of these cloned cDNAs, including all cDNAs that could be differentiated by their electrophoretic mobilities, were determined. The results of this analysis are summarized in Table 1. The majority of these cDNAs contained the 108-bp sequence corresponding to the region between the sequence complementary to the 160KPS primer and the sequence 5'-UUUUUAU-3' at the end point of complementarity between the RNA and the DNA template strand (Fig. 2). The last uridylate residue in the RNA and its corresponding adenylate in the template strand of the DNA were each designated -1 relative to the position of the major 3' end of the mRNA. Downstream of the -1 nucleotide, each of these cDNAs had a run of adenylates (17–40) corresponding to the 3' poly(A) tails of the RNAs. The difference between the lengths of the cloned inserts and the lengths of the PCR generated fragments may reflect an instability of long poly(A) stretches in the bacterial plasmids, as demonstrated by the failure to recover any cloned cDNA containing a poly(A) sequence of >40 residues. Previous analyses indicated that the *ati*

TABLE 1

## Nucleotide Sequences at the 3' Ends of cDNAs

Sequence at the 3' end of the cDNA	Number of isolates
Cowpox virus <i>ati</i> gene RNAs	
(-15) CACAAAAGAUUUUAUA <sub>(17)</sub> <sup>a</sup>	1
(-15) CACAAAAGAUUUUAUA <sub>(18)</sub>	2
(-15) CACAAAAGAUUUUAUA <sub>(18)</sub> <sup>b</sup> -69 A to G	2
(-15) CACAAAAGAUUUUAUA <sub>(19)</sub>	2
(-15) CACAAAAGAUUUUAUA <sub>(20)</sub>	1
(-15) CACAAAAGAUUUUAUA <sub>(22)</sub> <sup>b</sup> -60 U to C	2
(-15) CACAAAAGAUUUUAUA <sub>(26)</sub>	1
(-15) CACAAAAGAUUUUAUA <sub>(29)</sub>	3
(-15) CACAAAAGAUUUUAUA <sub>(40)</sub>	1
(-15) CACAAAAGAUUUUAUA <sub>(18)</sub>	2
(-15) CAAAA <u>CA</u> <sub>(19)</sub>	1
(-15) CACAAAAGAUUUUAUC..UUGUUA <sub>(31)</sub> (last U at +50)	1
Vaccinia virus <i>ati</i> gene RNAs	
(-15) CACAAAAGAUUUUAUA <sub>(17)</sub>	1
(-15) CACAAAAGAUUUUAUA <sub>(18)</sub>	1
(-15) CACAAAAGAUUUUAUA <sub>(21)</sub> <sup>b</sup> -16 U to C	1
(-35) CA <sub>(36)</sub>	1

<sup>a</sup> Number of adenylates.

<sup>b</sup> Base change from sequence in the viral DNA. Other base changes from sequence in the viral DNA are underlined.

mRNAs were ~4.5 kb long (Patel and Pickup, 1987). Therefore, taking into account the 5' poly(A) sequences of ~20 nucleotides and the specific 3' end of these mRNAs, this suggests that most of these mRNAs each contains ~100 adenylates immediately downstream of the RNA cleavage site.

Four of the 20 characterized cDNAs that were derived from the 3' ends of *ati* mRNAs differed from the other cDNAs. Two of these cDNAs contained the sequence ATT at +1 to +3. This sequence was apparently derived in a template-independent manner, presumably during reverse transcription or PCR amplification, because the corresponding sequence in the DNA template strand is 5'-CCG-3'. One cDNA was apparently derived from an *ati* mRNA whose 3' end was 50 nucleotides downstream of the usual 3' end site. Similarly, a fourth cDNA was obtained whose sequence suggested a 3' end at -14 followed by the sequence A<sub>(3)</sub>CA<sub>(19)</sub>. The C may also have been added in a template-independent manner, perhaps misincorporated for an A during the cloning procedure. The predicted 3' ends at +50 and -14 represent either artifacts of the cloning procedure or uncommon *ati* RNAs because RNAs whose 3' ends corresponded to either of these positions were not detected by S1 nuclease protection analyses (Antczak *et al.*, 1992). One cDNA was obtained that was derived not from the *ati* gene but rather from a 26-nucleotide sequence within

the coding region of the gene encoding the VP39 subunit of the poly(A) polymerase (Gershon *et al.*, 1991). This cDNA product was probably generated through annealing of the oligo(dT) primer to a region containing seven As and to the homology between the 3' end of the 160KPS primer and an 8-nucleotide sequence 11 nucleotides upstream of the seven As.

Analysis of the 3' ends of cDNAs of the vaccinia virus *ati* mRNAs revealed similar 3' end structures (Table 1) consistent with the identical nature of the sequences of the DNAs of viruses of these two types in the region containing the signal directing the RNA 3' end formation.

Collectively, these results confirm that the majority of viral *ati* mRNAs contain 3' poly(A) sequences commencing at the AX cleavage site. This is consistent with the model of RNA 3' end formation involving cleavage of precursor RNAs followed by the 3' polyadenylation of the 5' cleavage products (Antczak *et al.*, 1992).

#### A 43-nucleotide *cis*-acting element within the 345-bp *AluI*-*XbaI* fragment directs RNA 3' end formation.

To determine the identity of the *cis*-acting signal directing the sequence-specific RNA 3' end formation, portions of the 345-bp *AluI*-*XbaI* fragment containing the sequence corresponding to the end of the RNAs were tested for the ability to direct RNA 3' end formation. For this purpose, 13 recombinant vaccinia viruses were generated, each containing the chloramphenicol acetyltransferase (CAT) gene, under the control of the cowpox virus *ati* gene promoter, upstream of either the intact 345-bp *AluI*-*XbaI* fragment, or variants of this fragment, as described in Figs. 1-3. Late RNAs were extracted from cells infected with these recombinant viruses. The CAT gene RNAs produced by these viruses were analyzed by hybridization as shown in Fig. 3. The results demonstrated that the *AluI*-*XbaI* fragment contains the information necessary to direct the formation of sequence specific 3' ends (lane a). Accordingly, the *cis*-acting element directing RNA 3' end formation was designated the AX element (Antczak *et al.*, 1992). Moreover, sequence analysis of cDNA copies of the 3' ends of these CAT transcripts showed that the ends of the transcripts were identical to those of the authentic mRNAs encoding the ATI protein (data not shown).

A series of deletion variants of the *AluI*-*XbaI* fragment was examined to locate the sequences that direct RNA 3' end formation (Fig. 3). Parenthetically, it should be noted that deleted regions are necessarily replaced by flanking vector sequences, which may have some influence on 3' end formation, depending on their nature and proximity to the cleavage site. Deletion of sequences to within 15 bp upstream of the cleavage site did not affect RNA 3' end formation, whereas deletion of sequences to 1 bp upstream of the cleavage site removed necessary sequence information (Fig. 3, lanes b-e). As expected,

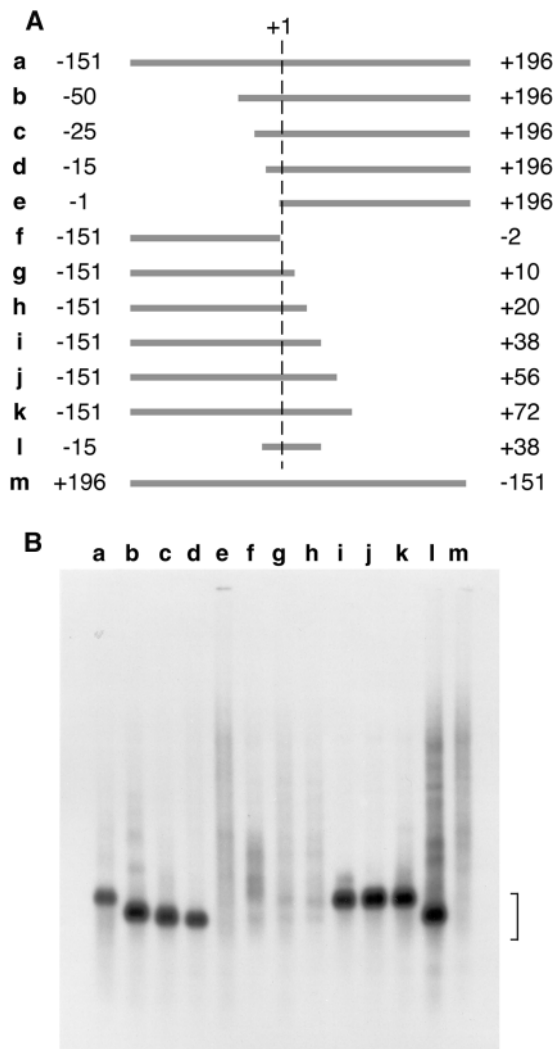


**FIG. 3.** Deletion analysis of the 345-nucleotide *AluI*-*XbaI* fragment containing the AX element. (A) Diagram showing the portions of the *AluI*-*XbaI* fragment that were inserted downstream of a copy of the CAT gene under the transcriptional control of the promoter element of the *ati* gene, as described above (Figs. 1F and 2), into the genomes of vaccinia viruses. The vertical broken line corresponds to the position of the cleavage site (between nucleotides -1 and +1). The *AluI*-*XbaI* fragment extends 151 nucleotides upstream of the cleavage site and 196 nucleotides downstream of the cleavage site. The full-length *AluI*-*XbaI* fragment was inserted into the genomes of vaccinia either in the same orientation as the CAT gene (a) or in the opposite orientation (m). (b-l) Truncated versions of the *AluI*-*XbaI* fragment (numbers indicate the extent of the truncation with respect to the cleavage site). (B) Northern blot analyses of the CAT RNAs containing the variants of the 345-nucleotide *AluI*-*XbaI* fragment. At late times after infection, polyadenylated RNAs extracted from cells infected with these recombinant vaccinia viruses were resolved by agarose gel electrophoresis and then transferred to a nylon membrane. The immobilized RNAs were probed with single-stranded RNA probes specific for the coding region of the CAT gene. The constructs contained in the viruses are as described in A. The CAT transcripts that were cleaved are of defined lengths; these cleaved RNAs are visualized as discrete bands within the bracketed region. The sizes of these RNAs differ according to the different lengths of the *AluI*-*XbaI* fragment upstream of the cleavage site in each virus.

deletions at the 5' end of the *AluI*-*XbaI* fragment result in correspondingly shorter CAT RNAs. Analysis of the effects of 3' deletions of the *AluI*-*XbaI* fragment showed that RNA 3' end formation was not affected by the substitution of sequences to within 38 bp downstream of the 3' end site, but substitution to +20 bp abrogated RNA 3' end formation (Fig. 3, lanes f-k). A deletion variant containing the 53-nucleotide sequence from -15 to +38 contained sufficient information to direct RNA 3' end formation (Fig. 3, lane l).

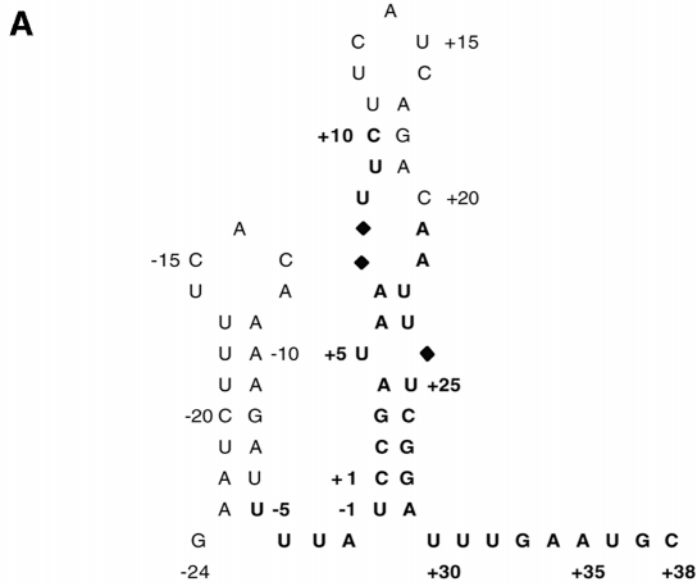
Additional constructs demonstrated other properties of the AX element. Reversal of the orientation of the *AluI*-*XbaI* fragment abrogated its ability to direct RNA 3' end formation (Fig. 3, lane m). Thus the AX element functions in one orientation only. Tandem duplication of the *cis*-acting element, as shown in Fig. 1G (a construct containing the -50 to +196 truncated *AluI*-*XbaI* fragment upstream of a full-length copy of the *AluI*-*XbaI* fragment), resulted in the formation of ends corresponding to the upstream element (Fig. 3, lane b), consistent with RNA 3' end formation by endoribonucleolytic cleavage, rather than by stabilization against degradation from 3' exonucleases.

As Fig. 3 shows, when the AX element in these variants is functional, almost all of the CAT RNAs have defined 3' ends corresponding to the AX cleavage site, and when the AX element is not functional, the detectable CAT RNAs are heterogeneous in length. However, in all lanes, minor CAT RNA species can be detected on extended exposure, suggesting that multiple longer, but much less abundant, CAT RNAs also are present in the infected cells. These may correspond to some of the minor CAT RNA species detected in the cDNA analysis described above. Currently, it is unclear whether the 3' ends of these species are generated by RNA processing or transcriptional termination.

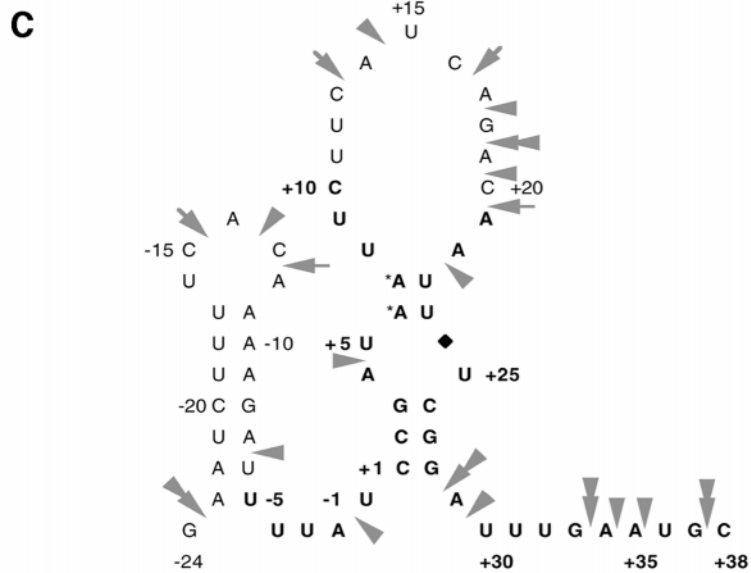
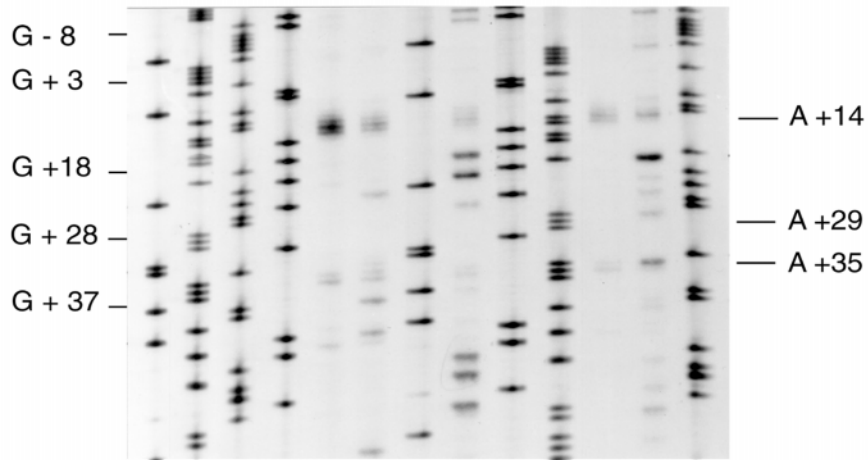
To define the AX element more precisely, a second series of deletion mutants was constructed as described in Fig. 4A. The same methodology was used to generate this second set of deletions of the *AluI*-*XbaI* fragment as was used in the first set.

The results of this analysis are shown in Fig. 4. The 5' deletion of sequences to -10 or -5 did not prevent RNA 3' end formation (Fig. 4B, lanes a and b), suggesting that the 5' boundary of the AX element is between -5 and -1. The 3' deletion of sequences to +35, +30, or +25 less clearly defined the downstream boundary of the AX element. Although deletion to +30 resulted in the abrogation of RNA 3' end formation at the AX site (Fig. 4B, lane d), substitutions to +35 and +25 still resulted in the accumulation of RNAs with 3' ends corresponding to the AX cleavage site (Fig. 4B, lanes c and e). However, the CAT RNAs of these latter two deletion mutants were less abundant than CAT RNAs of other mutants that enabled cleavage at the AX element. This was demonstrated (Fig. 4B) by comparison of the amounts of CAT RNAs using





**B**      G T A C 1 2 G 3 C T 4 5 A



adopt or maintain this predicted structure, unless either RNA—protein or additional RNA—RNA interactions stabilized such a conformation.

Second, the secondary structure of a 260-base RNA transcript containing the AX element was analyzed by partial digestion of the RNA *in vitro* with the structure-sensitive ribonucleases A, T1, and U2, as described previously (Colvin and Garcia-Blanco, 1992). The results of this analysis are shown in Fig. 5B and summarized in Fig. 5C. This analysis supported the positioning of residues C1 to G3 and C26 to G28 within a stem, but a major RNase U2 cleavage site after A29 (Fig. 5B, lane 5) indicated that any stem containing these residues was shorter than in the computer-generated alignment. Very weak digestion occurred after G28 (Fig. 5B, lane 2), indicating some accessibility in this region. There also was very weak cleavage after A4 (Fig. 5B, lane 5), which was predicted to lie next to a bulge. An unpaired region larger than that predicted was present in the *in vitro* transcript as indicated by cleavages after G18 (Fig. 5B, lane 2), A14, A17, and A19 (Fig. 5B, lane 5). Major cleavage sites for RNase A occurred at C13 and C16 (Fig. 5B, lane 3), which were predicted to lie within the loop of the hairpin, but only weak cleavage was visible at C20, and none was visible at C10. Cleavage was not detected after residues A6 and A7 (Fig. 5B, lane 5), which were included in the upper part of the hypothetical stem (Fig. 5A), but we cannot conclude that these two residues are base-paired or unpaired because a strong stop for the reverse transcriptase at these residues may have masked RNase digestion at these sites. Similar results were obtained using a longer transcript from plasmid p2098 as substrate (data not shown) when the transcripts were digested with RNase A and T1 in the same buffer used to obtain virus-induced RNA cleavage of the AX element contained in this RNA (Antczak *et al.*, 1992). Using a series of enzyme dilutions and 1 pmol of RNA, cleavage was obtained using 5 units of T1 and  $10^{-3}$  and  $10^{-4}$  units of RNase A. The results were the same as for the p1730 transcript experiments shown in Fig. 5, except that cleavage was relatively weaker at G37, stronger at C20, and very weak at C26. Although these data provide

some support for the predicted stem-loop formation between residues  $-23$  and  $-5$ , upstream of the AX element, they provide little support for intrinsic stem-loop formation in the  $-5$  to  $+38$  region that composes the AX element.

Collectively, these results suggest that the AX element consists of at least two separate *cis*-acting subelements with an intervening 10-nucleotide region. Currently, it is unclear whether these two subelements function independently or in association with each other. These analyses do not suggest that the two subelements associate directly with each other *in vitro*, but at this point we cannot rule out the possibility that such an association occurs in the cell in the presence of other factors involved in RNA 3' end formation.

## DISCUSSION

Previously, we demonstrated that a 345-nucleotide sequence within the primary transcript of the *ati* gene contained a *cis*-acting element, designated the AX element, capable of directing site-specific RNA cleavage *in vitro* (Antczak *et al.*, 1992). This study has defined the AX element as a 43-nucleotide *cis*-acting element containing the information necessary to direct the efficient production of late RNAs with 3' ends corresponding to those of the *ati* mRNAs.

In this study, we examined the effects of mutagenesis of the AX element on RNA 3' end formation in the context of virus-infected cells. These analyses indicate that the AX element consists of at least two subelements: one containing the cleavage site, and the other positioned downstream of the cleavage site (Fig. 4C). In the cell, portions of these two subelements may be able to interact through base-pairing between complementary regions, particularly if these associations are stabilized by viral or cell-encoded proteins. Alternatively, the two subelements may act as independent binding sites for one or more factors effecting the RNA 3' end formation. Precedents for control elements of the latter type include the *cis*-acting signals directing endoribonucleolytic processing and polyadenylation of mammalian and yeast

**FIG. 5.** Analysis of the potential secondary structure of the AX element. (A) Potential base-pairing within the essential region of an uncleaved AX element and flanking sequences as predicted by the RNA fold algorithm (Zuker and Stiegler, 1981; Zuker *et al.*, 1991), indicating the potential for the formation of an AU-rich stem-loop structure involving elements of the two separated components of the AX element (nucleotides  $-5$  to  $+10$  and nucleotides  $+21$  to  $+38$  with respect to the RNA cleavage site). (B) *In vitro* synthesized transcripts of the AX element were incubated in buffer either with or without a ribonuclease, and products of partial cleavage were analyzed by primer extension. Sequence reactions are designated by letters, and assay samples are designated by numbers. Assay samples show the products of primer extension after incubation of the RNA in the presence of: lane 1, RNase buffer alone; lane 2, RNase T1; lane 3, RNase A; lane 4, RNase U2 buffer; lane 5, RNase U2. Sequence ladders were derived for the complementary strand but are labeled to correspond to the RNA strand to allow easier comparison with assay samples (e.g., the ladder after lane 2 corresponds to the sequence of the antisense DNA strand obtained using dideoxy C). Because the ribonucleases cleave after the target nucleotide, products of reverse transcription end one base below the position of actual cleavage, causing a shift of one base with respect to the sequence ladder; kinase-labeling of the primer used for reverse transcription shifts down the product an additional half-base. (C) Structure predicted from the ribonuclease analyses. Cleavage sites are indicated as follows: RNase T1 (double arrowhead), RNase A (arrow), and RNase U2 (single arrowhead). The asterisks indicate sites where cleavage was not determined because partial termination of primer extension occurred at these sites even in the absence of ribonuclease treatment. Cleavage of the AX-element by the virus-induced ribonuclease occurs between residues designated  $-1$  and  $+1$ .



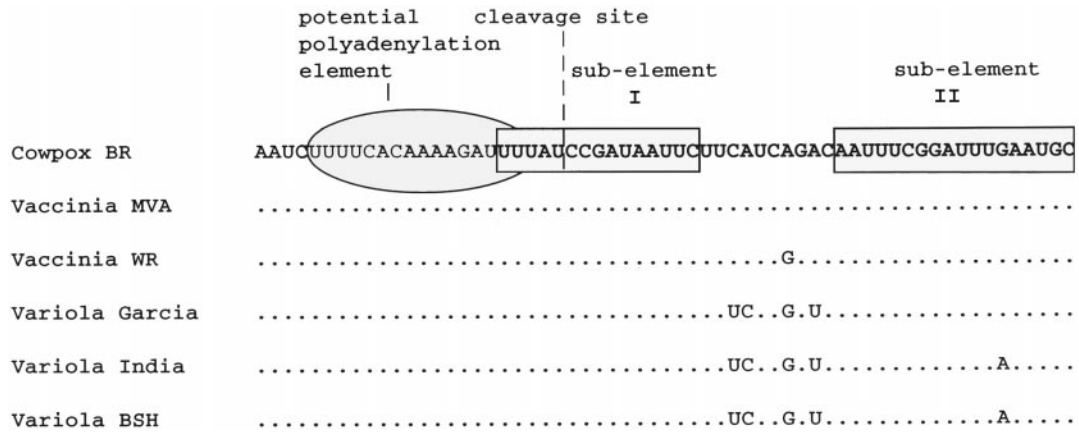


FIG. 6. Comparison of the cowpox virus AX element with the predicted corresponding regions of other orthopoxvirus RNAs. The sequence of the primary *ati* RNA transcript is shown, indicating the potential polyadenylation motif (Deng *et al.*, 1997), the RNA cleavage site (Antczak *et al.*, 1992), and AX subelements I and II (boxed). This sequence is aligned with the predicted RNA sequences of: vaccinia virus MVA (Antoine *et al.*, 1998), which is identical to the corresponding sequence of vaccinia virus Copenhagen (Goebel *et al.*, 1990), vaccinia virus WR (Amegadzie *et al.*, 1991), variola virus Garcia-1966 (GenBank accession number X76268), variola virus India-1967 (Shchelkunov *et al.*, 1993), and variola virus Bangladesh-1975 (Massung *et al.*, 1994). Identities are indicated by a dot, and differences are indicated by the base substitution.

RNA polymerase II transcripts (reviewed by Colgan and Manley, 1997; Wahle and Keller, 1996). In mammalian systems, these control elements comprise at least two sequence elements: the highly conserved AAUAAA sequence, usually  $\sim 10$ – $30$  nucleotides upstream of the RNA cleavage site, and less well defined U- or GU-rich sequences downstream of the RNA cleavage site. Sequences upstream of the AAUAAA element may also contribute to the efficiency of RNA 3' end formation. The AAUAAA element contributes to the binding of the cleavage and polyadenylation specificity factor (CPSF), whereas the GU-rich element contributes through binding the cleavage stimulation factor (CstF). These consensus AAUAAA and U or GU-rich sequences do not resemble the AX element either in their sequences or in their positions relative to the RNA cleavage site. This suggests that the 3' end formation of RNA polymerase II transcripts and the 3' end formation of viral *ati* mRNAs involve different factors, as might be expected, given both the cytoplasmic site of viral transcription and the use of virus-encoded enzymes for most other steps involved in the synthesis of viral RNAs. Indeed, the factors effecting AX-mediated RNA cleavage have been detected only in extracts of virus-infected cells (infected with cowpox or vaccinia virus) harvested during the late phase of virus replication (Antczak *et al.*, 1992), consistent with the involvement of virus-encoded proteins, but not excluding the involvement of host factors. Nonetheless, insofar as both processes of RNA 3' end formation involve endoribonucleolytic cleavage of primary transcripts, with subsequent polyadenylation of the 5' cleavage product, at sites determined by multiple *cis*-acting elements, the two processes are intriguingly similar.

The sequence analysis of cDNAs derived from the 3' ends of the *ati* mRNAs confirmed that these viral RNAs

are 3' polyadenylated after RNA cleavage. Recently, sequences governing efficient 3' polyadenylation of the early RNAs of vaccinia virus have been identified as comprising the sequence  $rU_{2n_{15}}U$  (Deng and Gershon, 1997; Deng *et al.*, 1997; Gershon and Moss, 1992). This sequence facilitates the association of the VP55 catalytic subunit of the poly(A) polymerase with the nascent 3' end of the RNA to be polyadenylated. This finding raises the question as to what sequences, if any, govern efficient 3' polyadenylation of the *ati* mRNAs. Inspection of the sequence upstream of the RNA cleavage site (Fig. 6) shows that consensus viral polyadenylation signals are present at  $-1$  and  $-21$ , together with several potential  $rU_{2n_{15}+}U$  elements, whose two uridylyate sites might be brought into appropriate positions relative both to each other, and to the nascent 3' end, by RNA folding. Accordingly, sequences of this type may constitute a third *cis*-acting subelement involved in late RNA 3' end formation. Further studies will be needed to determine the identities and roles played by these potential polyadenylation signals in RNA 3' end formation mediated by the AX element.

If the AX element is an important component of the *ati* transcriptional unit, then it might be expected to be a conserved feature of this unit. An almost identical AX element is present in the equivalent gene in the WR strain of vaccinia virus producing *ati* mRNAs that have a 3' end sequence identical to that of the cowpox virus *ati* gene mRNAs (Amegadzie *et al.*, 1991). This similarity of structure and function and the ability of vaccinia virus to effect RNA cleavage directed by the inserted cowpox virus *cis*-acting AX element (Antczak *et al.*, 1992) suggest that this process of RNA 3' end formation may be common among the poxviruses. Consistent with this suggestion, sequences almost identical to the AX element are

present in the genomes of several other orthopoxviruses, each of which contains a complete or partial version of the *ati* gene (Fig. 6). In these examples, where there are sequence differences, most of them occur between, and not within, the two AX subelements. This conservation might also occur independent of its role in RNA 3' end formation because the template strand of the AX element constitutes part of the coding strand of the *rpo132* gene. This explanation appears to be less likely because comparison with the *rpo132* genes of several less closely related poxviruses, capripoxvirus, molluscum contagiosum virus, and myxoma virus (Gershon *et al.*, 1989; Jackson *et al.*, 1996; Senkevich *et al.*, 1996), each of which lacks a convergently transcribed *ati* gene, reveals that the amino acid sequence of this region of the Rpo132 protein is not highly conserved. Therefore, the available sequence data suggest that the nucleotide sequence constituting the AX element may be conserved as part of the *ati* transcription unit.

The biological significance of the AX element-mediated RNA 3' end formation has yet to be determined. The *ati* gene is the most strongly expressed gene of the orthopoxviruses (Patel *et al.*, 1986). In part, this is attributable to efficient transcription from the *ati* gene promoter, but efficient site-specific 3' end formation may also contribute to the high level of expression of this gene. There are a number of ways in which this may occur.

First, some process of site-directed RNA 3' end formation is necessary or desirable, if only to ensure that mRNA 3' ends are downstream of the coding region, rather than within the coding region. It is noteworthy that the *ati* mRNAs are ~4.5 kb long, with little evidence of shorter, prematurely terminated transcripts (Amegadzie *et al.*, 1992; Patel and Pickup, 1987). Similarly, most other characterized viral late mRNAs, including those of heterogeneous lengths, are longer than their coding regions (Mahr and Roberts, 1984; Rosel and Moss, 1985; Weir and Moss, 1984), yet many of these mRNAs are shorter than the *ati* mRNAs. These features of late mRNAs are consistent with a mechanism in which (1) the transcriptional machinery is capable of transcribing kilobases of DNA with minimal adventitious termination of transcription, and (2) one or more *cis*-acting elements downstream of the coding region enable RNA 3' end formation. The AX element of the *ati* gene is such an element.

Second, the process of 3' end formation by RNA cleavage and polyadenylation may offer advantages to the virus over an alternative process of RNA 3' end formation by termination of transcription. This is especially likely if the latter process leads to the generation of viral mRNAs with heterogeneous 3' ends extending several kilobases downstream of the coding region of the gene. Such a process appears to be inefficient in the sense of unnecessary transcription of the genome. It is also a process potentially detrimental to the virus, both because it may

cause transcriptional interference with downstream genes (Adhya and Gottesman, 1982; Ink and Pickup, 1989; Proudfoot *et al.*, 1985) and because it may facilitate the generation of complementary RNAs with the potential to induce interferon-mediated antiviral effects and apoptosis (Hovanessian, 1991; Kibler *et al.*, 1997). Of course, post-transcriptional processing of *ati* mRNAs through the AX element still requires the production of transcripts complementary to those of the *rpo132* gene. However, again by analogy to RNA polymerase II transcription, the cleavage and polyadenylation of the *ati* primary RNAs may represent a cotranscriptional event that initiates the subsequent termination of transcription. Such a mechanism could minimize the extent of *ati* promoter-mediated transcription downstream of the AX element, generating only short, uncapped, nonpolyadenylated, 3' cleavage products that might be expected to be highly unstable. Several precedents for this kind of linkage between RNA 3' end processing and transcriptional termination have been described (Birse *et al.*, 1998; Connelly and Manley, 1988; Logan *et al.*, 1987). It remains to be seen if events of RNA cleavage, 3' polyadenylation, and the termination of transcription are normally coupled during the transcription of the *ati* gene.

Third, AX-mediated RNA 3' end formation may contribute to the efficiency of expression of the gene, through its effect on RNA stability. A number of studies have shown that the stability of the mRNA may be directly affected by the composition of the 3' untranslated region of the RNA (reviewed by Chen and Shyu, 1995; Ross, 1996). RNA 3' end formation at the AX element enables precise delimitation of the 3' untranslated region, which may enable the homogeneous *ati* mRNAs to each have similar stabilities governed by the presence (or absence) of a defined set of stability control elements. The structure of the 3' end might also affect the stability of the mRNA in other ways. For example, transcripts lacking a defined 3' end close to the end of the open reading frame might resemble defective mRNAs containing premature termination codons. Eukaryotic cells possess mechanisms for detecting and destroying such mRNAs (reviewed by Jacobson and Peltz, 1996; Maquat, 1995; Ruiz-Echevarria *et al.*, 1996, 1998; Zhang *et al.*, 1995). Therefore, viral RNAs lacking long untranslated 3' ends may also be less susceptible to degradation by mechanisms of this type.

Fourth, a colocalization of the *cis*-acting elements directing cleavage with the *cis*-acting elements directing polyadenylation may enable optimal production of 3' polyadenylated RNAs. In this way, the AX element may affect both transcriptional efficiency and stability of the RNA through its positioning of the RNA 3' end, and its potential effects on 3' polyadenylation.

Accordingly, the AX element, and sequences adjacent to the 3' end generated by RNA cleavage at the AX element are likely to contribute to the control of expression of the *ati* gene. RNA 3' end formation mediated by

the AX element may also have an effect on the expression of genes downstream of the *ati* gene, perhaps minimizing potential adverse effects of high levels of overlapping transcription from this gene.

These potential effects of AX-mediated RNA 3' end formation on *ati* gene transcription and expression suggest that similar processes may be used to regulate the expression of other viral genes. Further analyses of the AX element, the elements directing the 3' end formation of other late RNAs, and the factors interacting with these elements will help to determine whether the AX element-mediated RNA 3' end formation provides a paradigm for the mechanism of 3' end formation of other poxvirus late RNAs.

## METHODS

### Cells and viruses

Monolayers of 143 human osteosarcoma cells [thymidine kinase negative (TK<sup>-</sup>)] were maintained in Eagle's minimal essential medium (MEM; BioWhittaker, Walkersville, MD) supplemented with 5% FBS. The Brighton Red strain of cowpox virus (CPV), the WR strain of vaccinia virus, and their derivatives, were used for these studies. The bacterial plasmid pGEM3Z (Promega, Madison, WI) and its derivatives were selected and propagated in *E. coli* JM109.

### cDNA synthesis and PCR

The synthesis and PCR amplification of cDNA derived from the 3' termini of CPV *ati* gene transcripts were performed according to Kawasaki (1990). Reverse transcription was performed using a 33-base single-stranded (ss) DNA primer designated "160KdT," which consisted of the sequence 5'-GCCTGCAGGCGGC-CGCTTTTTTTTTTTTTTTTTT-3'. This primer was designed to promote reverse transcription of RNA molecules polyadenylated at their 3' termini via the 17 Ts located at the 3' end of the primer; in addition, it possessed a 5' "adapter" sequence containing *Pst*I and *Not*I restriction sites used for cloning the PCR-amplified cDNA. For reverse transcription, 0.5  $\mu$ g of the 160KdT primer and 1  $\mu$ g of total RNA, purified as described by Chomczynski and Sacchi (1987) from CPV-infected cells, were dissolved in 10  $\mu$ l of water, heated at 95°C for 3 min, and immediately cooled on ice. To this mixture was added 10  $\mu$ l of buffer yielding a 20- $\mu$ l reaction containing PCR buffer [20 mM Tris-HCl (pH 8.3 at 23°C), 50 mM KCl, 2.5 mM MgCl<sub>2</sub>, 100 mg BSA/ml]; 1 mM concentration of each of dGTP, dATP, dCTP, and dTTP; 2 mM DTT, 20 units of RNasin (Promega); and 400 units of Moloney murine leukemia virus reverse transcriptase (Life Technologies, Gaithersburg, MD). The reaction was incubated at 23°C for 10 min, 42°C for 30 min, and 55°C for 30 min; reverse transcription was subsequently terminated by incubation at 95°C

for 5 min. Specific amplification of cDNAs derived from the 3' termini of CPV *ati* gene transcripts was obtained using a PCR procedure (Kawasaki, 1990) with two unique ss DNA primers. The first primer, designated "160KPS," consisted of the 28-base sequence 5'-GCTCTAGA-GAGTTAAATGCCTCAGACGC-3', which contained a 5' *Xba*I restriction site (for cloning) and a 20-base 3' sequence (underlined) identical to a sequence located in the CPV genome ~405 bp downstream of the end of the region encoding the Ati protein. Because it was the same sense as *ati* mRNA, the primer would be complementary to cDNA derived by reverse transcription of *ati* gene transcripts that extended >425 bp downstream from the 3' end of the *ati* protein coding sequence and was designed to specifically prime second-strand synthesis from such cDNA molecules. The second primer, designated "160K3PR," was a 13-mer with the sequence 5'-GCCTGCAGGCGGC-3'. This primer was identical in sequence to the first 13 nucleotides at the 5' end of the reverse transcription primer, 160KdT, and was used to prime synthesis of strands during PCR amplification that were complementary to full-length strands derived by second-strand synthesis. Thus full-length, PCR-amplified duplex DNA derived in this way would possess an *Xba*I site at one end and *Pst*I and *Not*I sites at the opposite end. PCR was performed as follows: the 20- $\mu$ l reverse transcription reaction described above was diluted to a final reaction volume of 100  $\mu$ l containing 1 $\times$  PCR buffer; 0.2 mM concentration of each of dGTP, dATP, dCTP, and dTTP; 0.4 mM DTT; 2.5 units of *Taq* DNA polymerase (AmpliTaq; Perkin-Elmer Cetus, Foster City, CA); and 25 pmol each of the primers 160KPS and 160K3PR. The reaction was subjected to 30 cycles of incubation at 95°C for 30 s and 37°C for 1 min, with temperature increases and declines between the two plateaus occurring at the rates of ~1°/s and ~0.3°/s, respectively.

### Cloning and sequence analysis of cDNAs derived from the 3' termini of cowpox and vaccinia virus *ati* mRNAs

PCR products were recovered and digested with *Pst*I and *Xba*I. The *Pst*I-*Xba*I digestion products were resolved by electrophoresis in 8% polyacrylamide gel buffered with TBE and visualized by staining with ethidium bromide. Digestion products ranged in size from ~125 to 620 bp. The region of the gel containing fragments in this size range was sliced into eight sections (fractionating the smallest from the largest DNAs). The slices were excised, and the DNAs present in each slice were recovered by electroelution and then concentrated by ethanol precipitation. The recovered fragments were ligated into the unique *Pst*I and *Xba*I sites in the multiple cloning region of pGEM3Z, and the resulting ligation products were used to transform *E. coli* JM109 cells. The size of inserts in resultant plasmids was determined by agarose

TABLE 2

## Plasmid and Virus Constructions

Coordinates of the insert	Plasmid	Virus
-151 to +196	p1277	A415
-50 to +196	p2108	A471
-25 to +196	p1428	A472
-15 to +196	p1438	A480
-1 to +196	p1432	A477
-151 to -2	p1433	A478
-151 to +10	p1439	A481
-151 to +20	p1440	A485
-151 to +38	p1488	A494
-151 to +56	p1469	A491
-151 to +72	p2104	A470
-15 to +38	p1507	A501
-151 to +196 (reverse orientation)	p1278	A416
-10 to +196	p1516	A629
-5 to +196	p1515	A630
-151 to +35	p1618	A631
-151 to +30	p1518	A632
-151 to +25	p1517	A634
-50 to +196 sm at +1 to +5	p1617	A635
-50 to +196 sm at +6 to +10	p1612	A636
-50 to +196 sm at +11 to +15	p1613	A637
-50 to +196 sm at +16 to +20	p1614	A638
-50 to +196 sm at +21 to +25	p1615	A639
-50 to +196 sm at +26 to +30	p1616	A640

*Note.* Numbers relate to nucleotide number relative to the RNA cleavage site as shown in Figure 2. The last 6 constructs have scanning mutations (sm) at the indicated positions.

gel analysis of the products of digestion of the plasmid DNAs with *Pst*I and *Xba*I. The sequences of the inserts were determined by primer-directed sequencing of alkali-denatured plasmids using T7 DNA polymerase (Sequenase; U.S. Biochemicals, Cleveland, OH) according to the procedures of Tabor and Richardson (1987; 1990).

### Construction of deletion mutations

The insertion vector (p1275) used to insert the various mutated versions of the AX element into vaccinia virus genomes (as depicted in Fig. 1) was constructed as follows. The *Hind*III fragment of plasmid p1245 (Patel *et al.*, 1988) containing the CAT gene under the transcriptional control of the late promoter of the *ati* gene, inserted into the TK gene within the *Hind*III J fragment of vaccinia virus DNA, was inserted into the *Hind*III site of p1247 (pUC19 lacking the polylinker region except for the *Eco*RI and *Hind*III sites). This created the vector p1275, which contains a single *Bam*HI site at the 3' end of the CAT open reading frame.

Most of the variant AX elements were constructed by PCR with primers containing *Bam*HI sites to permit insertion into the p1275 DNA. The template used for the PCR was DNA of plasmid p2070, a pUC19 vector containing the 600-bp *Alu*I fragment spanning the AX element. The coordinates of the mutated elements (also see

Fig. 2), together with the designations of the insertion plasmids and recombinant viruses into which they were inserted, are presented in Table 2. The orientation and nucleotide sequence of each PCR-generated DNA ligated into p1275 were confirmed before these DNAs were inserted into the recombinant viruses. Plasmids p2104 and p2108 were generated not by PCR but rather by cloning the *Cl*aI-*Xba*I and *Alu*I-*Nsi*I subfragments of the *Alu*-*Xba*I fragment (containing the AX element) into the *Bam*HI site of plasmid p1275. In plasmid p2108, a complete AX element was inserted in tandem downstream of the *Alu*I-*Nsi*I subfragment.

### Construction of scanning mutations

Six scanning mutations were made within the 30 bases immediately downstream of the AX cleavage site. For each of the six mutations, different sets of five consecutive bases were substituted with the sequence GTACA using site-directed mutagenesis. Briefly, an oligonucleotide containing the altered bases flanked by wild-type sequence was annealed to ss M13mp18 vector DNA into which the 223-bp *Alu*I-*Nsi*I fragment (fragment derived from plasmid p2108) spanning the AX element had been cloned using *Bam*HI linkers (generating a phage designated mCAE). Using the oligonucleotide as primer, a complementary strand containing dCMP $\alpha$ S was synthesized using the Sculptor In Vitro Mutagenesis Kit (Amersham, Arlington Heights, IL). The wild-type strand was nicked and digested with exonuclease, and a second strand was synthesized complementary to the mutated strand. Competent *E. coli* cells were transformed with RF DNA, phages were recovered, and mutations were verified by sequence analysis. RF DNA containing the desired mutation was extracted from phage-infected cells and digested with *Bam*HI, and the mutated insert was cloned into p1275. Each of these plasmids containing the mutated sequence was inserted into the genome of a recombinant vaccinia virus as described below.

### Construction of recombinant vaccinia viruses

Human 143 cells ( $3.5 \times 10^6$  cells) in 60-mm tissue culture dishes were infected with vaccinia virus at an m.o.i. of 0.01. At 1 h postinfection, infected cell monolayers were washed twice with MEM and then overlaid with 3 ml of serum-free MEM. Then, 10  $\mu$ g of purified plasmid DNA were diluted in 100  $\mu$ l of H<sub>2</sub>O and mixed with 50  $\mu$ l of Lipofectin Reagent (Life Technologies, Gaithersburg, MD) plus 50  $\mu$ l of H<sub>2</sub>O. After 15-min incubation at room temperature, the mixture was added to the cells. After overnight incubation, 3 ml of MEME containing 10% serum was added. Lysates of infected cell were prepared at 2 days postinfection and used to infect subconfluent monolayers of human TK-143 cells. TK<sup>-</sup> recombinant

viruses were selected as described previously (Mackett *et al.*, 1984).

### RNA hybridization analyses

**Preparation of poly(A)<sup>+</sup> RNA.** Monolayers of  $2 \times 10^7$  human 143 cells grown in 150-mm tissue culture dishes were infected with vaccinia or cowpox viruses, at an m.o.i. of 10 pfu/cell. At 14 h postinfection, cell monolayers were washed twice with cold PBS, and cells were scraped with a rubber policeman into 5 ml of cold PBS and centrifuged to pellet cells. The pellet was resuspended in 1 ml of lysis solution (4 M guanidine thiocyanate, 0.025 M sodium acetate, pH 7, 0.05% Sarkosyl, 0.72%  $\beta$ -mercaptoethanol) and vortexed. DNA was sheared by passing the lysate several times through a 22-gauge needle. Then, 200  $\mu$ l of 2 M sodium acetate, pH 4.0, was added, followed by 1 ml of buffered phenol and 420  $\mu$ l of chloroform. After a 15-min incubation on ice, lysates were centrifuged for 15 min at 3000 rpm (Sorvall H1000B rotor). RNA was precipitated from the aqueous phase by the addition of 1 volume of isopropanol. After centrifugation, the RNA pellet was resuspended in 150  $\mu$ l of lysis solution and reextracted by the addition of 250  $\mu$ l of phenol and 100  $\mu$ l of chloroform, followed by a 5-min centrifugation at 12,000g. RNA was reprecipitated in 2.5 volumes of ethanol. The air-dried RNA pellet was resuspended in 250  $\mu$ l of DEPC-H<sub>2</sub>O containing 0.2% SDS. Poly(A)<sup>+</sup> RNA was isolated using the PolyATract mRNA isolation system II (Promega) according to the manufacturer's instructions. After drying, final RNA pellets were resuspended in DEPC-H<sub>2</sub>O.

**Gel electrophoresis and RNA blotting.** Gels (1.5% agarose) containing 2% formaldehyde were prepared in 1× MOPS buffer (0.02 M MOPS, 0.005 M sodium acetate, 0.001 M EDTA). RNA samples (5  $\mu$ g) were mixed with loading buffer and electrophoresed at 25 mA for 4–5 h. Gels were soaked in H<sub>2</sub>O for 2 × 10 min and then blotted onto nylon membranes by capillary transfer using 10× SSC as transfer buffer.

**Probe synthesis.** Radiolabeled RNA transcripts complementary to either the CAT or *ati* gene transcripts were prepared either from plasmid p1328, a pT7–1 vector (U.S. Biochemicals) containing the *Hind*III–*Bam*HI fragment containing the CAT gene, obtained from plasmid p862, a derivative of pSV2-catS (Gorman *et al.*, 1982) constructed by Dr. E. Linney (Duke University, Durham, NC); or from plasmid p1624, a pGEM4Z vector containing a 1.5-kb *Eco*RI–*Hinc*II fragment (encompassing the region at the 5′ end of the *ati* gene) of plasmid p2031 (Patel and Pickup, 1987), which is a 2-kb *Acc*I fragment containing the 5′ end of the *ati* gene inserted into the *Eco*RI site of pUC9. Probes were prepared using the Riboprobe system (Promega) according to the manufacturer's instructions.

**Hybridization with labeled probe.** Membranes containing the immobilized RNAs were prehybridized for  $\geq 4$  h at 55°C in hybridization solution (50% formamide, 50 mM NaPO<sub>4</sub>, pH 6.5, 5× SSC, 1× Denhardt's solution, 200  $\mu$ g/ml denatured salmon sperm DNA). Fresh hybridization solution was added before the addition of labeled probe. After overnight incubation at 55°C, membranes were washed in 65°C in 1× SSC and 0.1% SDS and then in 0.1× SSC and 0.1% SDS. The dried membranes were exposed to autoradiographic film.

### RNA secondary structure analysis

**Plasmid construction.** For the construction of p1730, the 260-bp *Nsi*I–*Xba*I fragment of the AX element was inserted into *Bam*HI-digested pGEM4Z (Promega) using *Bam*HI linkers. The insert was oriented so that transcription from the T7 promoter yielded a transcript of the same sense as the *ati* gene transcript.

**In vitro transcription.** Plasmid p1730 DNA was linearized by digestion with *Eco*RI, which cuts downstream of the insert within the vector polylinker. The linearized plasmid was gel purified, and 2.5  $\mu$ g was used as template in an *in vitro* transcription reaction with T7 RNA polymerase according to the manufacturer's instructions (Promega). After the reaction, RNA transcripts were treated with RQ1 DNase I (Promega), extracted with phenol–chloroform, and ethanol precipitated. The RNA pellet was resuspended in DEPC-treated H<sub>2</sub>O. This transcript was 320 bases long, with 260 bases derived from the insert, and the remainder from flanking vector sequences.

**Partial digestion with ribonucleases.** Three structure-sensitive enzymes were chosen: RNase A, which cleaves after ss pyrimidines and has some preference for C over T residues; RNase T1, which cleaves after ss G residues; and RNase U2, which cleaves after ss purines with preference for A residues (Knapp, 1989). RNA transcripts were diluted to 1 pmol/ $\mu$ l (0.1  $\mu$ g of RNA was calculated to be equivalent to 1 pmol based on a full-length transcript of 320 bases) in RNase assay buffer (70 mM HEPES, pH 7.9, 10 mM MgCl<sub>2</sub>, 200 mM KCl), heated to 55°C for 10 min, and cooled slowly to room temperature to allow renaturation. Optimal concentrations of ribonucleases and incubation times were established in preliminary assays. For digestion with RNase A or T1, the assay mixture consisted of 1 pmol of RNA, 1 mM DTT, and 10<sup>–3</sup> units of RNase A (U.S. Biochemicals) or 5 units of RNase T1 (Boehringer-Mannheim, Indianapolis, IN) in a final volume of 20  $\mu$ l of 1× RNase assay buffer. Assay samples were incubated at 37°C for 5 min. For digestion with RNase U2, 1 pmol of RNA was incubated with 0.05 unit of RNase U2 (Calbiochem, San Diego, CA) in 20 mM sodium acetate, pH 5.2, containing 10 mM MgCl<sub>2</sub> and 100 mM KCl, at 37°C for 5 min. For controls, transcripts were incubated in the same conditions but without the

addition of enzymes. After the appropriate incubation period with the ribonuclease, samples were immediately chilled, and 4  $\mu\text{g}$  of tRNA in 80  $\mu\text{l}$  of  $\text{H}_2\text{O}$  was added. Immediately, protein was extracted by phenol-chloroform extraction, after which the RNA was recovered by ethanol precipitation.

**Primer extension.** Primer 160MSB (3'-GCTACCTA-CAAAGCAATG-5'), which maps 72 nucleotides downstream of the AX cleavage site, was radiolabeled at the 5' end using [ $\gamma$ - $^{32}\text{P}$ ]ATP and T4 polynucleotide kinase using standard procedures (Sambrook *et al.*, 1989). Then, 0.5 pmol of end-labeled 160MSB was annealed to RNase-digested RNA substrate in a final volume of 6  $\mu\text{l}$  by heating at 50°C for 10 min, followed by 10 min of slow cooling. For reverse transcription, annealed primer-RNA duplexes were added to a reaction mixture containing Superscript buffer (0.5 M Tris-HCl, pH 8.3, 0.075 M KCl, 3 mM  $\text{MgCl}_2$ ); 10 mM DTT; 1 mM concentration of each of dCTP, dATP, dTTP, and dGTP; 8 mM sodium pyrophosphate; 1  $\mu\text{l}$  (40 units) of RNA Guard (Amersham Pharmacia, Piscataway, NJ); and 200 units of Superscript reverse transcriptase (Life Technologies, Gaithersburg, MD) in a final volume of 20  $\mu\text{l}$ . Reactions were incubated at 37°C for 30 min, mixed with loading buffer, and electrophoresed in a denaturing 6% polyacrylamide gel. Sizes of primer extension products were determined from sequence reaction products synthesized using p1730 as template, oligonucleotide 160MSB as primer, and labeled by the incorporation of [ $^{35}\text{S}$ ]dATP.

## ACKNOWLEDGMENTS

This work was supported by U.S. Public Health Service Grants R01-AI23886, R01-AI32982, and 5T32CA09111 (J.B.A.) from the National Institutes of Health. D.J.P. is a member of the Duke University Comprehensive Cancer Center, whose shared core facilities were used in this study.

## REFERENCES

- Adhya, S., and Gottesman, M. (1982). Promoter occlusion: Transcription through a promoter may inhibit its activity. *Cell* **29**, 939-944.
- Amegadzie, B. Y., Holmes, M. H., Cole, N. B., Jones, E. V., Earl, P. L., and Moss, B. (1991). Identification, sequence, and expression of the gene encoding the second-largest subunit of the vaccinia virus DNA-dependent RNA polymerase. *Virology* **180**, 88-98.
- Amegadzie, B. Y., Sisler, J. R., and Moss, B. (1992). Frame-shift mutations within the vaccinia virus A-type inclusion protein gene. *Virology* **186**, 777-782.
- Antczak, J. B., Patel, D. D., Ray, C. A., Ink, B. S., and Pickup, D. J. (1992). Site-specific RNA cleavage generates the 3' end of a poxvirus late mRNA. *Proc. Natl. Acad. Sci. USA* **89**, 12033-12037.
- Antoine, G., Scheiflinger, F., Dorner, F., and Falkner, F. G. (1998). The complete genomic sequence of the modified vaccinia Ankara strain: comparison with other orthopoxviruses. *Virology* **244**, 365-396.
- Archard, L. C., Mackett, M., Barnes, D. E., and Dumbell, K. R. (1984). The genome structure of cowpox virus white pock variants. *J. Gen. Virol.* **65**, 875-886.
- Birse, C. E., Minvielle-Sebastia, L., Lee, B. A., Keller, W., and Proudfoot, N. J. (1998). Coupling termination of transcription to messenger RNA maturation in yeast. *Science* **280**, 298-301.
- Chen, C. Y., and Shyu, A. B. (1995). AU-rich elements: Characterization and importance in mRNA degradation. *Trends Biochem. Sci.* **20**, 465-470.
- Chomczynski, P., and Sacchi, N. (1987). Single-step method of RNA isolation by acid guanidinium thiocyanate-phenol-chloroform extraction. *Anal. Biochem.* **162**, 156-159.
- Colgan, D. F., and Manley, J. L. (1997). Mechanism and regulation of mRNA polyadenylation. *Genes Dev.* **11**, 2755-2766.
- Colvin, R. A., and Garcia-Blanco, M. A. (1992). Unusual structure of the human immunodeficiency virus type 1 trans-activation response element. *J. Virol.* **66**, 930-935.
- Connelly, S., and Manley, J. L. (1988). A functional mRNA polyadenylation signal is required for transcription termination by RNA polymerase II. *Genes Dev.* **2**, 440-452.
- Deng, L., Beigelman, L., Matulic-Adamic, J., Karpeisky, A., and Gershon, P. D. (1997). Specific recognition of an  $\text{rU}_2\text{-N}_{15}\text{-rU}$  motif by VP55, the vaccinia virus poly(A) polymerase catalytic subunit. *J. Biol. Chem.* **272**, 31542-31552.
- Deng, L., and Gershon, P. D. (1997). Interplay of two uridylate-specific RNA binding sites in the translocation of poly(A) polymerase from vaccinia virus. *EMBO J.* **16**, 1103-1113.
- Deng, L., Hagler, J., and Shuman, S. (1996). Factor-dependent release of nascent RNA by ternary complexes of vaccinia RNA polymerase. *J. Biol. Chem.* **271**, 19556-19562.
- Deng, L., and Shuman, S. (1996). An ATPase component of the transcription elongation complex is required for factor-dependent transcription termination by vaccinia RNA polymerase. *J. Biol. Chem.* **271**, 29386-29392.
- Deng, L., and Shuman, S. (1998). Vaccinia NPH-I, a DEXH-box ATPase, is the energy coupling factor for mRNA transcription termination. *Genes Dev.* **12**, 538-546.
- Devereux, J., Haeberli, P., and Smithies, O. (1984). A comprehensive set of sequence analysis programs for the VAX. *Nucleic Acids Res.* **12**, 387-395.
- Frohman, M. A., Dush, M. K., and Martin, G. R. (1988). Rapid production of full-length cDNAs from rare transcripts: amplification using a single gene-specific oligonucleotide primer. *Proc. Natl. Acad. Sci. USA* **85**, 8998-9002.
- Frohman, M. A. (1990). RACE: Rapid amplification of cDNA ends. In "PCR Protocols: A Guide to Methods and Applications" (Innis, M. A., Gelfand, D. H., Sninsky, J. J., and White, T. J., eds.) pp 28-38, Academic Press, San Diego.
- Gershon, P. D., Ahn, B. Y., Garfield, M., and Moss, B. (1991). Poly(A) polymerase and a dissociable polyadenylation stimulatory factor encoded by vaccinia virus. *Cell* **66**, 1269-1278.
- Gershon, P. D., Ansell, D. M., and Black, D. N. (1989). A comparison of the genome organization of capripoxvirus with that of the orthopoxviruses. *J. Virol.* **63**, 4703-4708.
- Gershon, P. D., and Moss, B. (1992). Transition from rapid processive to slow nonprocessive polyadenylation by vaccinia virus poly(A) polymerase catalytic subunit is regulated by the net length of the poly(A) tail. *Genes Dev.* **6**, 1575-1586.
- Goebel, S. J., Johnson, G. P., Perkus, M. E., Davis, S. W., Winslow, J. P., and Paoletti, E. (1990). The complete DNA sequence of vaccinia virus. *Virology* **179**, 247-266, 517-563.
- Gorman, C. M., Moffat, L. F., and Howard, B. H. (1982). Recombinant genomes which express chloramphenicol acetyltransferase in mammalian cells. *Mol. Cell. Biol.* **2**, 1044-1051.
- Hovanessian, A. G. (1991). Interferon-induced and double-stranded RNA-activated enzymes: A specific protein kinase and 2',5'-oligoadenylate synthetases. *J. Interferon Res.* **11**, 199-205.
- Ink, B. S., and Pickup, D. J. (1989). Transcription of a poxvirus early gene is regulated both by a short promoter element and by a transcriptional termination signal controlling transcriptional interference. *J. Virol.* **63**, 4632-4644.
- Jackson, R. J., Hall, D. F., and Kerr, P. J. (1996). Construction of recombinant myxoma viruses expressing foreign genes from different in-

- tergenic sites without associated attenuation. *J. Gen. Virol.* **77**, 1569–1575.
- Jacobson, A., and Peltz, S. W. (1996). Interrelationships of the pathways of mRNA decay and translation in eukaryotic cells. *Annu. Rev. Biochem.* **65**, 693–739.
- Kawasaki, E. S. (1990). Amplification of RNA. In "PCR Protocols: A Guide to Methods and Applications" (Innis, M. A., Gelfand, D. H., Sninsky, J. J., and White, T. J., Eds.), pp. 21–27, Academic Press, San Diego.
- Kibler, K. V., Shors, T., Perkins, K. B., Zeman, C. C., Banaszak, M. P., Biesterfeldt, J., Langland, J. O., and Jacobs, B. L. (1997). Double-stranded RNA is a trigger for apoptosis in vaccinia virus-infected cells. *J. Virol.* **71**, 1992–2003.
- Knapp, G. (1989). Enzymatic approaches to probing of RNA secondary and tertiary structure. *Methods Enzymol.* **180**, 192–212.
- Logan, J., Falck-Pedersen, E., Darnell, J. E., Jr., and Shenk, T. (1987). A poly(A) addition site and a downstream termination region are required for efficient cessation of transcription by RNA polymerase II in the mouse  $\beta^{\text{maj}}$ -globin gene. *Proc. Natl. Acad. Sci. USA* **84**, 8306–8310.
- Mackett, M., Smith, G. L., and Moss, B. (1984). General method for production and selection of infectious vaccinia virus recombinants expressing foreign genes. *J. Virol.* **49**, 857–864.
- Mahr, A., and Roberts, B. E. (1984). Arrangement of late RNAs transcribed from a 7.1-kilobase EcoRI vaccinia virus DNA fragment. *J. Virol.* **49**, 510–520.
- Maquat, L. E. (1995). When cells stop making sense: Effects of nonsense codons on RNA metabolism in vertebrate cells. *RNA* **1**, 453–465.
- Massung, R. F., Liu, L. I., Qi, J., Knight, J. C., Yuran, T. E., Kerlavage, A. R., Parsons, J. M., Venter, J. C., and Esposito, J. J. (1994). Analysis of the complete genome of smallpox variola major virus strain Bangladesh-1975. *Virology* **201**, 215–240.
- Moss, B. (1996) Poxviridae: The viruses, and their replication. In "Virology" (Fields, B. N., Knipe, D. M., Howley, P. M., et al., Eds.), pp. 2637–2671, Philadelphia, Lippincott-Raven Publishers.
- Parsons, B. L., and Pickup, D. J. (1990). Transcription of orthopoxvirus telomeres at late times during infection. *Virology* **175**, 69–80.
- Patel, D. D., and Pickup, D. J. (1987). Messenger RNAs of a strongly-expressed late gene of cowpox virus contain 5'-terminal poly(A) sequences. *EMBO J.* **6**, 3787–3794.
- Patel, D. D., and Pickup, D. J. (1989). The second largest subunit of the poxvirus RNA polymerase is similar to the corresponding subunits of procaryotic and eucaryotic RNA polymerases. *J. Virol.* **63**, 1076–1086.
- Patel, D. D., Pickup, D. J., and Joklik, W. K. (1986). Isolation of cowpox virus A-type inclusions and characterization of their major protein component. *Virology* **149**, 174–189.
- Patel, D. D., Ray, C. A., Drucker, R. P., and Pickup, D. J. (1988). A poxvirus-derived vector that directs high levels of expression of cloned genes in mammalian cells. *Proc. Natl. Acad. Sci. USA* **85**, 9431–9435.
- Pickup, D. J., Ink, B. S., Parsons, B. L., Hu, W., and Joklik, W. K. (1984). Spontaneous deletions and duplications of sequences in the genome of cowpox virus. *Proc. Natl. Acad. Sci. USA* **81**, 6817–6821.
- Proudfoot, N. J., Gil, A., and Whitelaw, E. (1985). Studies on messenger RNA 3' end formation in globin genes: A transcriptional interference model for globin gene switching. *Prog. Clin. Biol. Res.* **191**, 49–65.
- Rohrmann, G., Yuen, L., and Moss, B. (1986). Transcription of vaccinia virus early genes by enzymes isolated from vaccinia virions terminates downstream of a regulatory sequence. *Cell* **46**, 1029–1035.
- Rosel, J., and Moss, B. (1985). Transcriptional and translational mapping and nucleotide sequence analysis of a vaccinia virus gene encoding the precursor of the major core polypeptide 4b. *J. Virol.* **56**, 830–838.
- Ross, J. (1996). Control of messenger RNA stability in higher eukaryotes. *Trends Genet.* **12**, 171–175.
- Ruiz-Echevarria, M. J., Czaplinski, K., and Peltz, S. W. (1996). Making sense of nonsense in yeast. *Trends Biochem. Sci.* **21**, 433–438.
- Ruiz-Echevarria, M. J., Gonzalez, C. I., and Peltz, S. W. (1998). Identifying the right stop: determining how the surveillance complex recognizes and degrades an aberrant mRNA. *EMBO J.* **17**, 575–589.
- Sambrook, J., Fritsch, E. F., and Maniatis, T. (1989). "Molecular Cloning: A Laboratory Manual," 2nd ed. Cold Spring Harbor Laboratory Press, Cold Spring Harbor, New York.
- Senkevich, T. G., Bugert, J. J., Sisler, J. R., Koonin, E. V., Darai, G., and Moss, B. (1996). Genome sequence of a human tumorigenic poxvirus: Prediction of specific host response-evasion genes. *Science* **273**, 813–816.
- Shchelkunov, S. N., Marennikova, S. S., Blinov, V. M., Resenchuk, S. M., Tetmenin, A. V., Chizhikov, V. E., Gutorov, V. V., Safronov, P. F., Kurmanov, R. K., and Sandakchiev, L. S. (1993). Entire coding sequence of the variola virus. *Dokl. Akad. Nauk.* **328**, 629–632.
- Shuman, S., Broyles, S. S., and Moss, B. (1987). Purification and characterization of a transcription termination factor from vaccinia virions. *J. Biol. Chem.* **262**, 12372–12380.
- Shuman, S., and Moss, B. (1988). Factor-dependent transcription termination by vaccinia virus RNA polymerase: Evidence that the cis-acting termination signal is in nascent RNA. *J. Biol. Chem.* **263**, 6220–6225.
- Tabor, S., and Richardson, C. C. (1987). DNA sequence analysis with a modified bacteriophage T7 DNA polymerase. *Proc. Natl. Acad. Sci. USA* **84**, 4767–4771.
- Tabor, S., and Richardson, C. C. (1990). DNA sequence analysis with a modified bacteriophage T7 DNA polymerase: Effect of pyrophosphorylation and metal ions. *J. Biol. Chem.* **265**, 8322–8328.
- Wahle, E., and Keller, W. (1996). The biochemistry of polyadenylation. *Trends Biochem. Sci.* **21**, 247–250.
- Weinrich, S. L., and Hruby, D. E. (1987). Noncoordinate regulation of a vaccinia virus late gene cluster. *J. Virol.* **61**, 639–645.
- Weinrich, S. L., Niles, E. G., and Hruby, D. E. (1985). Transcriptional and translational analysis of the vaccinia virus late gene L65. *J. Virol.* **55**, 450–457.
- Weir, J. P., and Moss, B. (1984). Regulation of expression and nucleotide sequence of a late vaccinia virus gene. *J. Virol.* **51**, 662–669.
- Yuen, L., and Moss, B. (1987). Oligonucleotide sequence signaling transcriptional termination of vaccinia virus early genes. *Proc. Natl. Acad. Sci. USA* **84**, 6417–6421.
- Zhang, S., Ruiz-Echevarria, M. J., Quan, Y., and Peltz, S. W. (1995). Identification and characterization of a sequence motif involved in nonsense-mediated mRNA decay. *Mol. Cell. Biol.* **15**, 2231–2244.
- Zuker, M., Jaeger, J. A., and Turner, D. H. (1991). A comparison of optimal and suboptimal RNA secondary structures predicted by free energy minimization with structures determined by phylogenetic comparison. *Nucleic Acids Res.* **19**, 2707–2714.
- Zuker, M., and Stiegler, P. (1981). Optimal computer folding of large RNA sequences using thermodynamics and auxiliary information. *Nucleic Acids Res.* **9**, 133–148.